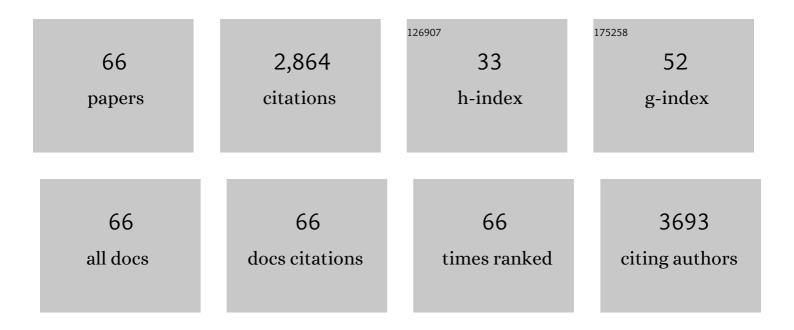
Zhi-Yi Hu

List of Publications by Year in descending order

Source: https://exaly.com/author-pdf/7837541/publications.pdf Version: 2024-02-01



<u>7нг-Уг Ни</u>

#	Article	IF	CITATIONS
1	Tailoring CuO nanostructures for enhanced photocatalytic property. Journal of Colloid and Interface Science, 2012, 384, 1-9.	9.4	162
2	Novel 3DOM BiVO ₄ /TiO ₂ nanocomposites for highly enhanced photocatalytic activity. Journal of Materials Chemistry A, 2015, 3, 21244-21256.	10.3	139
3	Nano-single crystal coalesced PtCu nanospheres as robust bifunctional catalyst for hydrogen evolution and oxygen reduction reactions. Journal of Catalysis, 2019, 375, 164-170.	6.2	133
4	3D Ferroconcrete‣ike Aminated Carbon Nanotubes Network Anchoring Sulfur for Advanced Lithium–Sulfur Battery. Advanced Energy Materials, 2018, 8, 1801066.	19.5	115
5	Oxygen-deficient titanium dioxide as a functional host for lithium–sulfur batteries. Journal of Materials Chemistry A, 2019, 7, 10346-10353.	10.3	109
6	BiVO4/3DOM TiO2 nanocomposites: Effect of BiVO4 as highly efficient visible light sensitizer for highly improved visible light photocatalytic activity in the degradation of dye pollutants. Applied Catalysis B: Environmental, 2017, 205, 121-132.	20.2	100
7	2D ZnO mesoporous single-crystal nanosheets with exposed {0001} polar facets for the depollution of cationic dye molecules by highly selective adsorption and photocatalytic decomposition. Applied Catalysis B: Environmental, 2016, 181, 138-145.	20.2	95
8	n-p Heterojunction of TiO2-NiO core-shell structure for efficient hydrogen generation and lignin photoreforming. Journal of Colloid and Interface Science, 2021, 585, 694-704.	9.4	91
9	MOF-derived nitrogen-doped core–shell hierarchical porous carbon confining selenium for advanced lithium–selenium batteries. Nanoscale, 2019, 11, 6970-6981.	5.6	83
10	In-Situ Growing Mesoporous CuO/O-Doped g-C ₃ N ₄ Nanospheres for Highly Enhanced Lithium Storage. ACS Applied Materials & Interfaces, 2019, 11, 32957-32968.	8.0	78
11	Spatial Heterojunction in Nanostructured TiO ₂ and Its Cascade Effect for Efficient Photocatalysis. Nano Letters, 2020, 20, 3122-3129.	9.1	74
12	One-Step Growth of Amorphous/Crystalline Ga ₂ O ₃ Phase Junctions for High-Performance Solar-Blind Photodetection. ACS Applied Materials & Interfaces, 2019, 11, 45922-45929.	8.0	67
13	One particle@one cell: Highly monodispersed PtPd bimetallic nanoparticles for enhanced oxygen reduction reaction. Nano Energy, 2014, 8, 214-222.	16.0	66
14	Hollow nitrogen-doped carbon/sulfur@MnO2 nanocomposite with structural and chemical dual-encapsulation for lithium-sulfur battery. Chemical Engineering Journal, 2020, 381, 122746.	12.7	66
15	Hierarchical Zeolite Single-Crystal Reactor for Excellent Catalytic Efficiency. Matter, 2020, 3, 1226-1245.	10.0	66
16	Carbon quantum dots modified TiO2 composites for hydrogen production and selective glucose photoreforming. Journal of Energy Chemistry, 2022, 64, 201-208.	12.9	63
17	Selenium clusters in Zn-glutamate MOF derived nitrogen-doped hierarchically radial-structured microporous carbon for advanced rechargeable Na–Se batteries. Journal of Materials Chemistry A, 2018, 6, 22790-22797.	10.3	62
18	Micronâ€ S ized Zeolite Beta Single Crystals Featuring Intracrystal Interconnected Ordered Macroâ€Mesoâ€Microporosity Displaying Superior Catalytic Performance. Angewandte Chemie - International Edition, 2020, 59, 19582-19591.	13.8	61

Zнı-Yı Hu

#	Article	IF	CITATIONS
19	Coproduction of hydrogen and lactic acid from glucose photocatalysis on band-engineered Zn1-xCdxS homojunction. IScience, 2021, 24, 102109.	4.1	61
20	Phase-junction Ag/TiO2 nanocomposite as photocathode for H2 generation. Journal of Materials Science and Technology, 2021, 83, 179-187.	10.7	52
21	Cocatalyzing Pt/PtO Phase-Junction Nanodots on Hierarchically Porous TiO ₂ for Highly Enhanced Photocatalytic Hydrogen Production. ACS Applied Materials & Interfaces, 2017, 9, 29687-29698.	8.0	51
22	A flexible, hierarchically porous PANI/MnO ₂ network with fast channels and an extraordinary chemical process for stable fast-charging lithium–sulfur batteries. Journal of Materials Chemistry A, 2020, 8, 2741-2751.	10.3	50
23	Type II heterojunction in hierarchically porous zinc oxide/graphitic carbon nitride microspheres promoting photocatalytic activity. Journal of Colloid and Interface Science, 2019, 538, 99-107.	9.4	49
24	Probing conducting polymers@cadmium sulfide core-shell nanorods for highly improved photocatalytic hydrogen production. Journal of Colloid and Interface Science, 2018, 521, 1-10.	9.4	48
25	Unprecedented and highly stable lithium storage capacity of (001) faceted nanosheet-constructed hierarchically porous TiO2/rGO hybrid architecture for high-performance Li-ion batteries. National Science Review, 2020, 7, 1046-1058.	9.5	46
26	Anion-Modulated Platinum for High-Performance Multifunctional Electrocatalysis toward HER, HOR, and ORR. IScience, 2020, 23, 101793.	4.1	45
27	Weaving 3D highly conductive hierarchically interconnected nanoporous web by threading MOF crystals onto multi walled carbon nanotubes for high performance Li–Se battery. Journal of Energy Chemistry, 2021, 59, 396-404.	12.9	43
28	Probing and suppressing voltage fade of Li-rich Li1.2Ni0.13Co0.13Mn0.54O2 cathode material for lithium-ion battery. Electrochimica Acta, 2019, 318, 875-882.	5.2	42
29	Atomic defects, functional groups and properties in MXenes. Chinese Chemical Letters, 2021, 32, 339-344.	9.0	40
30	A Stable, Reusable, and Highly Active Photosynthetic Bioreactor by Bio-Interfacing an Individual Cyanobacterium with a Mesoporous Bilayer Nanoshell. Small, 2015, 11, 2003-2010.	10.0	39
31	Revealing the Origin of Highly Efficient Polysulfide Anchoring and Transformation on Anionâ€5ubstituted Vanadium Nitride Host. Advanced Functional Materials, 2021, 31, 2008034.	14.9	39
32	Excellent Excitonic Photovoltaic Effect in 2D CsPbBr ₃ /CdS Heterostructures. Advanced Functional Materials, 2020, 30, 2006166.	14.9	38
33	Molybdenum disulfide quantum dots directing zinc indium sulfide heterostructures for enhanced visible light hydrogen production. Journal of Colloid and Interface Science, 2019, 551, 111-118.	9.4	35
34	Melamine-based polymer networks enabled N, O, S Co-doped defect-rich hierarchically porous carbon nanobelts for stable and long-cycle Li-ion and Li-Se batteries. Journal of Colloid and Interface Science, 2021, 582, 60-69.	9.4	34
35	Growing ordered CuO nanorods on 2D Cu/g-C3N4 nanosheets as stable freestanding anode for outstanding lithium storage. Chemical Engineering Journal, 2021, 407, 126941.	12.7	33
36	Synthesis of monodispersed CoMoO4 nanoclusters on the ordered mesoporous carbons for environment-friendly supercapacitors. Journal of Alloys and Compounds, 2019, 810, 151841.	5.5	28

Zнı-Yı Hu

#	Article	IF	CITATIONS
37	Nonlayered CdSe Flakes Homojunctions. Advanced Functional Materials, 2020, 30, 1908902.	14.9	28
38	A facile synthesis of Ag@PdAg core-shell architecture for efficient purification of ethene feedstock. Journal of Catalysis, 2019, 369, 440-449.	6.2	26
39	Effects of Nanostructure and Coating on the Mechanics of Carbon Nanotube Arrays. Advanced Functional Materials, 2016, 26, 1233-1242.	14.9	25
40	Interwoven scaffolded porous titanium oxide nanocubes/carbon nanotubes framework for high-performance sodium-ion battery. Journal of Energy Chemistry, 2021, 59, 38-46.	12.9	25
41	Diatom silica–titania photocatalysts for air purification by bio-accumulation of different titanium sources. Environmental Science: Nano, 2016, 3, 1052-1061.	4.3	24
42	Single-cell yolk-shell nanoencapsulation for long-term viability with size-dependent permeability and molecular recognition. National Science Review, 2021, 8, nwaa097.	9.5	23
43	Interface cation migration kinetics induced oxygen release heterogeneity in layered lithium cathodes. Energy Storage Materials, 2021, 36, 115-122.	18.0	23
44	Size effect of bifunctional gold in hierarchical titanium oxide-gold-cadmium sulfide with slow photon effect for unprecedented visible-light hydrogen production. Journal of Colloid and Interface Science, 2021, 604, 131-140.	9.4	23
45	Three-dimensional ordered hierarchically porous carbon materials for high performance Li-Se battery. Journal of Energy Chemistry, 2022, 68, 624-636.	12.9	23
46	Synergistic catalysis of Pd nanoparticles with both Lewis and Bronsted acid sites encapsulated within a sulfonated metal–organic frameworks toward one-pot tandem reactions. Journal of Colloid and Interface Science, 2019, 557, 207-215.	9.4	22
47	Cascade electronic band structured zinc oxide/bismuth vanadate/three-dimensional ordered macroporous titanium dioxide ternary nanocomposites for enhanced visible light photocatalysis. Journal of Colloid and Interface Science, 2019, 539, 585-597.	9.4	20
48	3D interconnected hierarchically macro-mesoporous TiO ₂ networks optimized by biomolecular self-assembly for high performance lithium ion batteries. RSC Advances, 2016, 6, 26856-26862.	3.6	19
49	Nickel clusters accelerating hierarchical zinc indium sulfide nanoflowers for unprecedented visible-light hydrogen production. Journal of Colloid and Interface Science, 2022, 608, 504-512.	9.4	17
50	Embedding tin disulfide nanoparticles in two-dimensional porous carbon nanosheet interlayers for fast-charging lithium-sulfur batteries. Science China Materials, 2021, 64, 2697-2709.	6.3	16
51	Hydrothermal and surfactant treatment to enhance the photocatalytic activity of hierarchically meso–macroporous titanias. Catalysis Today, 2013, 212, 89-97.	4.4	14
52	Probing the electrochemical behavior of {111} and {110} faceted hollow Cu ₂ O microspheres for lithium storage. RSC Advances, 2016, 6, 97129-97136.	3.6	13
53	Probing the Electron Beam-Induced Structural Evolution of Halide Perovskite Thin Films by Scanning Transmission Electron Microscopy. Journal of Physical Chemistry C, 2021, 125, 10786-10794.	3.1	13
54	Mesoporous Titanium Dioxide (TiO2) with hierarchically 3D dendrimeric architectures: Formation mechanism and highly enhanced photocatalytic activity. Journal of Colloid and Interface Science, 2013, 394, 252-262.	9.4	12

Zнı-Yı Hu

#	Article	IF	CITATIONS
55	Tris(trimethylsilyl) borate as electrolyte additive alleviating cathode electrolyte interphase for enhanced lithium-selenium battery. Electrochimica Acta, 2021, 393, 139042.	5.2	12
56	Realizing both n- and p-types of high thermoelectric performance in Fe1â^'xNixTiSb half-Heusler compounds. Journal of Materials Chemistry C, 2020, 8, 3156-3164.	5.5	11
57	The chain-mail Co@C electrocatalyst accelerating one-step solid-phase redox for advanced Li–Se batteries. Journal of Materials Chemistry A, 2022, 10, 8059-8067.	10.3	11
58	Tuning the structure of a hierarchically porous ZrO2 for dye molecule depollution. Microporous and Mesoporous Materials, 2012, 152, 110-121.	4.4	10
59	One-Step Microheterogeneous Formation of Rutile@Anatase Core–Shell Nanostructured Microspheres Discovered by Precise Phase Mapping. Journal of Physical Chemistry C, 2017, 121, 4443-4450.	3.1	9
60	Highly biocompatible Co@Silica@meso-Silica magnetic nanocarriers. Chemical Physics Letters, 2019, 717, 29-33.	2.6	9
61	Near-equiatomic high-entropy decagonal quasicrystal in Al20Si20Mn20Fe20Ga20. Science China Materials, 2021, 64, 440-447.	6.3	9
62	Hierarchical TiO2 microsphere assembled from nanosheets with high photocatalytic activity and stability. Chemical Physics Letters, 2020, 739, 136989.	2.6	8
63	The free-standing N-doped Murray carbon framework with the engineered quasi-optimal Se/C interface for high–Se-loading Li/Na–Se batteries at elevated temperature. Materials Today Energy, 2021, 21, 100808.	4.7	8
64	Gradient selenium-doping regulating interfacial charge transfer in zinc sulfide/carbon anode for stable lithium storage. Journal of Colloid and Interface Science, 2022, 619, 42-50.	9.4	5
65	Ï€-Ï€-Ï€ stacking for capturing-releasing Au clusters in meso-structured system. Chemical Physics Letters, 2018, 712, 134-138.	2.6	2
66	Atomic-resolution fine structure and chemical reaction mechanism of Gd/YbAl3 thermoelectric-magnetocaloric heterointerface. Journal of Alloys and Compounds, 2020, 831, 154722.	5.5	1